33. S. C. Solomon, J. W. Head, *J. Geophys. Res.* **84**, 1667 (1979).
34. A. B. Binder, M. A. Lange, *Moon* **17**, 29 (1977).
35. A. B. Binder, in *Origin of the Moon*, W. K. Hartmann, R. J. Phillips, G. J. Taylor Eds. (Lunar and Planetary Institute, Houston, TX, 1986), pp. 425–433.
36. We thank the three anonymous reviewers for helpful comments that improved the manuscript. We gratefully acknowledge the Lunar Orbiter Laser Altimeter team for the lunar topographic model and the LRO and LROC engineers and technical support personnel. This work was supported by the LRO Project, NASA grants NNX08AM73G and NNG07EK00C, and through Deutsches Zentrum für Luft- und Raumfahrt grant 50 OW 0901.

**Supporting Online Material**
www.sciencemag.org/cgi/content/full/329/5994/936/DC1
SOM Text
Figs. S1 to S4
Table S1

15 March 2010; accepted 8 July 2010
10.1126/science.1189590

# Drought-Induced Reduction in Global Terrestrial Net Primary Production from 2000 Through 2009

**Maosheng Zhao* and Steven W. Running**

Terrestrial net primary production (NPP) quantifies the amount of atmospheric carbon fixed by plants and accumulated as biomass. Previous studies have shown that climate constraints were relaxing with increasing temperature and solar radiation, allowing an upward trend in NPP from 1982 through 1999. The past decade (2000 to 2009) has been the warmest since instrumental measurements began, which could imply continued increases in NPP; however, our estimates suggest a reduction in the global NPP of 0.55 petagrams of carbon. Large-scale droughts have reduced regional NPP, and a drying trend in the Southern Hemisphere has decreased NPP in that area, counteracting the increased NPP over the Northern Hemisphere. A continued decline in NPP would not only weaken the terrestrial carbon sink, but it would also intensify future competition between food demand and proposed biofuel production.

Terrestrial ecosystems are a major sink in the global carbon cycle, sequestering carbon and slowing the increasing $CO_2$ concentration in the atmosphere (*1*). Terrestrial net primary production (NPP), the initial step of the carbon cycle in which carbon is fixed as biomass, increased from 1982 through 1999, in part due to eased climatic constraints on plant growth (*2*). The World Meteorological Organization (WMO), National Oceanic and Atmospheric Administration (NOAA), and NASA all reported that 2000 to 2009 was the warmest decade since instrumental measurements of temperatures began in the 1880s (*3*). We questioned whether the warming climate of the past decade continued to increase NPP, or if different climate constraints were more important.

Between 2000 and 2008, $CO_2$ emissions from fossil fuel combustion continued to increase at a rate consistent with the average of the highest-emissions family of scenarios, A1FI, used by the Intergovernmental Panel on Climate Change in the Fourth Assessment (*1*). Carbon-budget methods show that the land is becoming a stronger carbon sink, whereas large uncertainties exist in the partitioning of ocean and land carbon-sink components (*1*, *4*). Satellite data can generally provide realistic information on vegetation dynamics, including land cover change (*5*, *6*), disturbances, and recovery (*7*), which may help to reduce uncertainties in carbon-budget estimates. In this study, we investigate terrestrial NPP and climate variability over the past decade (2000 to 2009) by analyzing satellite data from the Moderate Resolution Imaging Spectroradiometer (MODIS) on board NASA's Terra satellite and global climate data.

We used the global MODIS NPP algorithm (*8*) [see supporting online material (SOM) text S1] to examine spatially explicit NPP changes from 2000 through 2009. We used collection 5 (C5) 8-day composite 1-km fraction of photosynthetically active radiation (FPAR) and leaf area index (LAI) data from the MODIS sensor (*9*) as remotely sensed vegetation property dynamic inputs to the algorithm. Data gaps in the 8-day temporal MODIS FPAR/LAI caused by cloudiness were filled with information from accompanying quality-assessment fields (SOM text S2) (*10*). For daily meteorological data required to drive the algorithm, we used a reanalysis data set from National Center for Environmental Prediction (NCEP) (SOM text S3) (*11*). A Palmer Drought Severity Index (PDSI) (*12*) at 0.5° resolution was used as a surrogate of soil moisture (*13*) to measure environmental water stress by combining information from both evaporation and precipitation (SOM text S4). A lower PDSI generally implies a drier climate.

Global NPP slightly decreased for the past decade by −0.55 Pg C (Fig. 1). Interannual variations of the global NPP were negatively correlated with the global atmospheric $CO_2$ growth rates (correlation coefficient $r = -0.89$, $p < 0.0006$) (Fig. 1) (*14*), suggesting that global terrestrial NPP is a major driver of the interannual $CO_2$ growth rate. Carbon isotopic measurements have indicated that the exchange of $CO_2$ with terrestrial ecosystems is the dominant cause of the $CO_2$ interannual growth rate (*15*). Though NPP is a part of carbon exchange between the land and atmosphere, the strong correlation may imply that the process of heterotrophic respiration depends ultimately on the substrate supply from NPP (*16*),

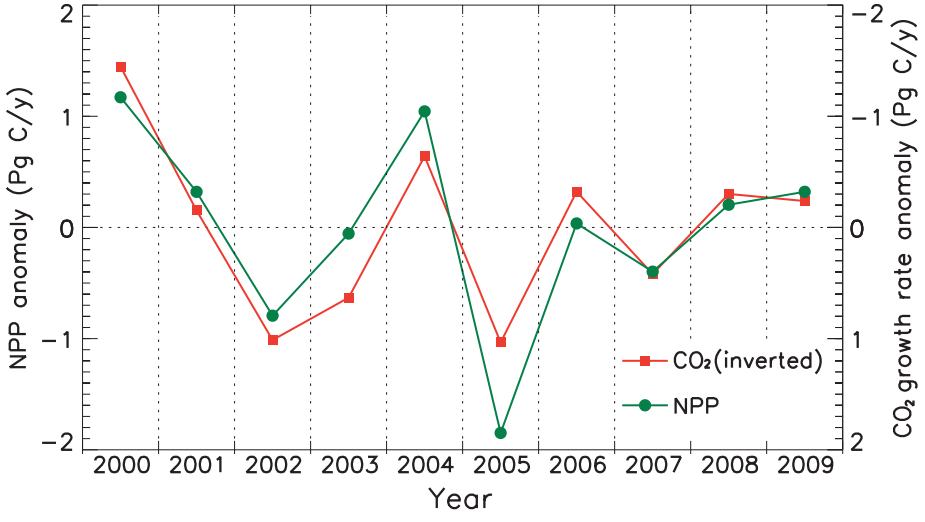


**Fig. 1.** Interannual variations from 2000 through 2009 in anomalies of annual total global terrestrial NPP (green circles) and inverted global atmospheric $CO_2$ annual growth rate [red squares and (*14*)]. Global average annual total NPP is 53.5 Pg C/yr.

Numerical Terradynamic Simulation Group, Department of Ecosystem and Conservation Sciences, the University of Montana, Missoula, MT 59812, USA.

*To whom correspondence should be addressed. E-mail: zhao@ntsg.umt.edu

as shown by the strong correlation between gross primary production (GPP) and ecosystem respiration derived from eddy-flux towers (*17*). Although also a major contributor, global fire emissions do not correlate as strongly as NPP with interannual $CO_2$ growth rate (SOM text S5) (*18*).

Regionally, negative annual NPP anomalies were mainly caused by large-scale droughts (fig. S7 and table S2). In 2000, droughts reduced NPP in North America and China; in 2002, droughts reduced NPP in North America and Australia; in 2003, drought caused by a major heat wave reduced NPP in Europe (*19*); in 2005, severe droughts in the Amazon (*20*), Africa, and Australia greatly reduced both regional and global NPP (Fig. 1 and fig. S7); and from 2007 through 2009, over large parts of Australia, continuous droughts reduced continental NPP.

NPP in the tropics (23.5°S to 23.5°N) explains 93% of variations in the global NPP, of which tropical rainforests explain 61% of global NPP variations (SOM text S8 and table S4). For the three major tropical rainforests (Amazon, Africa and Asia, see fig. S11), Amazon NPP alone explains 66% of the global NPP variations, though it accounts for only 14% of the global total, whereas the other two rainforests have no significant relation with global NPP variations (table S4). The growth of rainforests is mainly constrained by solar radiation due to severe cloudiness (fig. S10) (*2*, *21*), yet our study reveals that, except for rainforests in the islands of southeast Asia, the growth of rainforests in both the Amazon and Africa is also water limited (fig. S10 and table S5). Of the three major rainforests, only Africa had an increasing trend in NPP (0.189 Pg C per decade), which was mostly due to decreased vapor pressure deficit (VPD) (figs. S9 and S10). The other two had decreasing trends, with the Amazon at −0.424 Pg C per decade and Asia at −0.562 Pg C per decade (table S4). The decreased NPP in Asian rainforests was mainly caused by reductions in solar radiation, whereas reduction of NPP in the Amazon was mainly caused by increasing air temperature, which greatly increased autotrophic respiration (0.38 Pg C per decade), and also by a slight drying trend for the past decade, especially a severe drought in 2005 (figs. S12 and S14 and table S5).

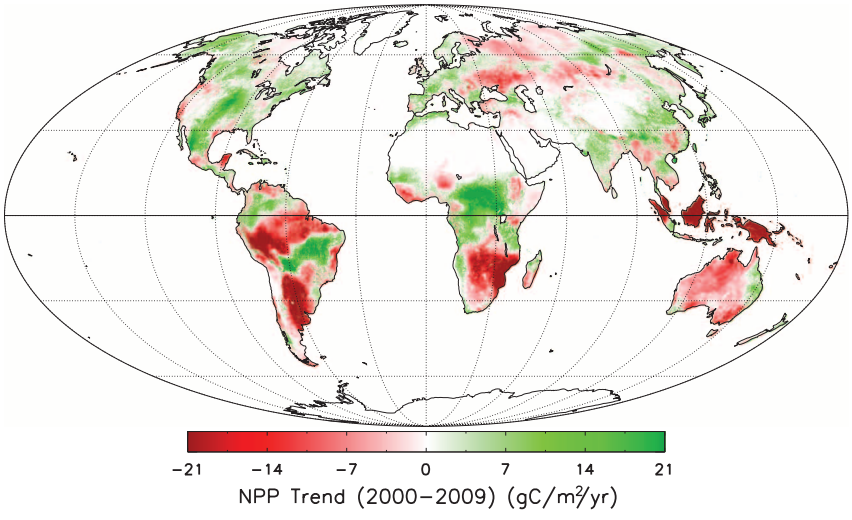


**Fig. 2.** Spatial pattern of terrestrial NPP linear trends from 2000 through 2009 (SOM text S1) (*8*, *10*).

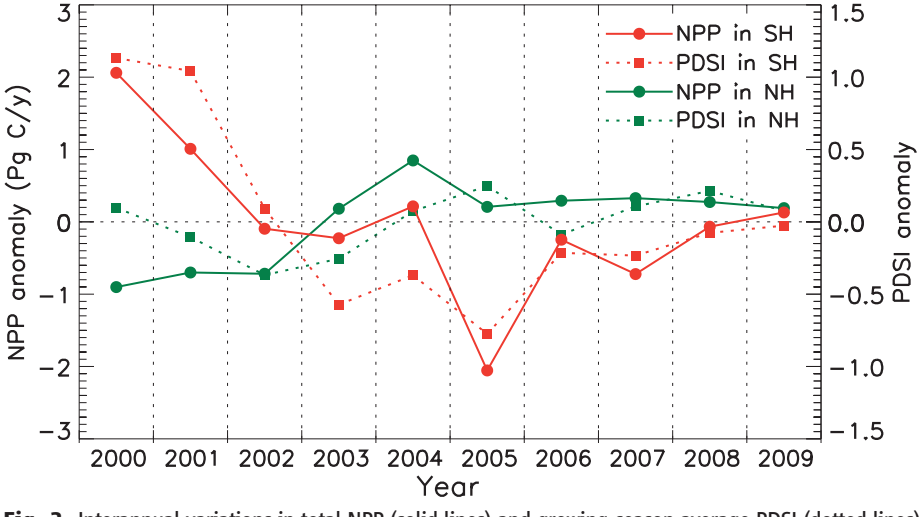


**Fig. 3.** Interannual variations in total NPP (solid lines) and growing-season average PDSI (dotted lines) over the NH (green) and SH (red) (SOM text S1 and S4).

There has been an ongoing debate about whether there was "green-up" of Amazon rainforests in the intense drought of 2005 (*22*, *23*). Hence, we examined MODIS C5 FPAR/LAI, related climate variables, and the resulting GPP and NPP over Amazon rainforests (SOM text S9). FPAR/LAI were higher in 2005, implying green-up of Amazon during drought (figs. S13 and S14). However, annual calculated NPP greatly decreased because of the combined effects of severe water stress and high-temperature–induced high-autotrophic respiration (figs. S13 and S14). The reduced NPP agrees with reported large decreases in plant growth (*20*). Though there was no green-up of C5 MODIS enhanced vegetation index (EVI) from the drought, there was no clear "browning" either (*23*). It is unclear what caused green-up of FPAR/LAI or the lack of browning of EVI; however, the reduction in NPP due to severe drought reveals that radiometric greenness is not necessarily a proxy for NPP in some cases. Therefore, remotely sensed NPP models should account for environment stresses and plant autotrophic respiration.

Figure 2 is the spatial pattern of NPP trends over the past decade: NPP increased over large areas in the Northern Hemisphere (NH) while decreasing in the Southern Hemisphere (SH). Over the NH, 65% of vegetated land area had increased NPP, including large areas of North America, Western Europe, India, China, and the Sahel. Regions with decreased NPP include Eastern Europe, central Asia, and high latitudes of west Asia. In the SH, 70% of vegetated land areas had decreased NPP, including large parts of South America, Africa, and Australia.

For northern high latitudes (>47.5°N), warming climate lengthens growing seasons, promoting plant growth (*24*). However, continuing warming may offset these benefits of an earlier spring and decrease carbon sequestration in a dryer summer and warmer autumn (*25*, *26*). Over the past decade, warming temperatures continued increasing NPP, albeit with a concurrent drying trend (figs. S8 and S9 and table S3). For northern mid-latitudes (22.5°N to 47.5°N), where there are large areas of short-rooted grasslands and croplands (fig. S2), water availability is a dominant control on plant growth. NPP had significant correlations with both growing-season total precipitation ($r = 0.96$, $p < 0.0001$) and average PDSI ($r = 0.76$, $p < 0.05$) (table S3), and a wet trend over the past decade increased NPP (fig. S8 and S9 and table S3). For the Tibet plateau with an average elevation of more than 4500 m, similar to the high latitudes, temperature is the

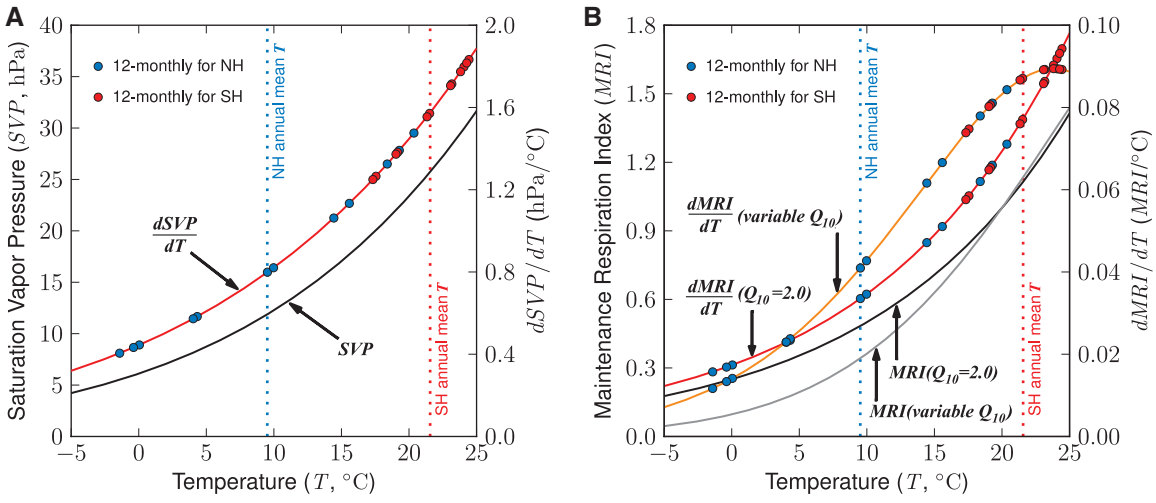


**Fig. 4.** SVP of the air as a function of T and derivative (**A**). MRI of plants as a function of T and derivative (**B**). Twelve-month average air temperature and derivatives of SVP and MRI with respect to T for both the NH and SH are also shown (table S6). For MRI, there are two equations, one with $Q_{10}$ (the difference in respiration rates over a 10°C interval) as a constant value of 2.0, and the other with a temperature-acclimated $Q_{10}$. Annual mean air temperature is 9.51°C for vegetated NH and 21.56°C for vegetated SH (table S6). See SOM text S10 for details of the equations.

dominant control on vegetation growth, and the recent warming climate increased NPP (Fig. 2 and figs. S9 and S10). For northern low latitudes (0°N to 22.5°N), reduced atmospheric VPD in Africa and India caused increased NPP in the zone (Fig. 2, fig. S9, and table S3). Overall, the NH had an increasing trend in NPP (Figs. 2 and 3, fig. S8, and table S3). Nitrogen deposition and fertilizer use also contributed to increased NPP in the NH (SOM text S5) (*27*).

For vegetated land areas in the SH, temperature is not a dominant factor controlling the length of growing season, as indicated by an average of only 7.5 days of snow cover annually, in contrast to 125 days in the NH, as observed by MODIS (fig. S3). Instead, high temperature causes high VPD and evaporation, generally reducing water availability for vegetation growth. Therefore, there is a significant correlation ($r = 0.87, p < 0.001$) between NPP and PDSI in the SH, though only a weak correlation ($r = 0.39, p < 0.27$) in the NH (Fig. 3). Despite increased precipitation over large parts of the SH (fig. S9 and table S3), the warming trend induced a much higher evaporative demand, leading to a drying trend (fig. S9 and table S3). As a result, NPP decreased because of warming-associated drying trends (Figs. 2 and 3, and figs. S9 and S10). Though NPP in the SH accounts for 41% of the global NPP, the stronger decreasing NPP trend (–1.83 Pg C per decade) counteracted a weaker increasing trend in the NH (1.28 Pg C per decade), resulting in a slight reduction in the global NPP (Figs. 1 and 3 and table S3).

To understand why there are different responses of NPP to a warming climate for two hemispheres, we examine two basic variables governing water and carbon fluxes: (i) saturation vapor pressure (SVP) and (ii) a maintenance respiration index (MRI) (SOM text S10). VPD is the difference between SVP and air vapor pressure, and SVP is a nonlinear function of air temperature (T). VPD is one major factor controlling surface evapotranspiration (ET) (*28*); thus, a high T value can increase both VPD and subsequent ET and lead to a dryer environment, eventually reducing NPP. MRI is a power function of T, and a warming climate will increase autotrophic respiration and potentially decrease NPP. Because of the amplification nature of these nonlinear functions to increasing temperature, for different temperature bases, the same increase in air temperature will have much higher increases of SVP and MRI at higher temperature bases than at lower temperatures. Figure 4 shows how SVP and MRI and their derivations respond to air temperatures of the two hemispheres. For vegetated land area, the annual mean T of the SH is more than 12°C higher than that of the NH. An equivalent increase of temperature will consequently have changes in SVP and MRI that are twice as strong in the SH than in the NH. Only during the NH summer (June, July, and August) will there be similar levels of response to warming compared to those of the SH. For the NH, summer is the major growing season; thus, NPP is also susceptible to warming and drought.

Recent simulations from coupled climate–carbon cycle models have shown that there is a positive feedback between the carbon cycle and the climate system (*29*–*31*), and also that future biological carbon sinks could eventually level off and subsequently decline to zero (*32*). Though Fig. 4 only shows MRI responses to temperature, soil respiration largely follows a similar nonlinear temperature response in these models (*31*). These nonlinear amplification responses of water and carbon processes to warming are the major mechanisms responsible for the positive feedback between the carbon and climate systems.

Though the warming climate during this period continuously increased NPP over areas of high latitude and high elevations, these warming-benefited areas only account for 16% of the global total NPP and 24% of global vegetated land area (SOM text S11). NPP over large land areas of lower latitude and altitude is negatively correlated with temperature (fig. S10A), mostly due to the warming-related increases in water stress and autotrophic respiration, especially for the SH ($r = -0.94$, $p < 0.0001$). Globally, interannual NPP is negatively correlated with air temperature over vegetated land ($r = -0.64, p < 0.05$) (table S3).

Over the past 10 years, large-scale periodic regional droughts and a general drying trend over the SH reduced global terrestrial NPP. Under a changing climate, severe regional droughts have become more frequent, a trend expected to continue for the foreseeable future (*13*, *33*, *34*). The warming-associated heat and drought not only decrease NPP, but also may trigger many more ecosystem disturbances (*6*, *35*, *36*), releasing carbon to the atmosphere (*18*, *37*). Reduced NPP potentially threatens global food security and future biofuel production and weakens the terrestrial carbon sink. Continuous global monitoring of NPP will be essential to determining whether the reduced NPP over the past 10 years is a decadal variation or a turning point to a declining terrestrial carbon sequestration under changing climate.

### References and Notes


1. C. Le Quéré *et al.*, *Nat. Geosci.* **2**, 831 (2009).
2. R. R. Nemani *et al.*, *Science* **300**, 1560 (2003).
3. The Web sites for the reports from WMO, NOAA and NASA, respectively, are www.wmo.int/pages/mediacentre/press_releases/pr_869_en.html, www.noaanews.noaa.gov/stories2009/20091208_globalstats.html, and www.nasa.gov/topics/earth/features/temp-analysis-2009.html.
4. K. L. Denman *et al.*, in *Climate Change 2007: The Physical Science Basis. Contribution of Working Group I to the Fourth Assessment Report of the Intergovernmental Panel on Climate Change*, S. Solomon *et al.*, Eds. (Cambridge Univ. Press, Cambridge, 2007), pp. 501–587.
5. M. C. Hansen *et al.*, *Proc. Natl. Acad. Sci. U.S.A.* **105**, 9439 (2008).
6. G. R. van der Werf, J. T. Randerson, L. Giglio, N. Gobron, A. J. Dolman, *Global Biogeochem. Cycles* **22**, GB3028 (2008).
7. D. J. Mildrexler, M. Zhao, S. W. Running, *Remote Sens. Environ.* **113**, 2103 (2009).

8. S. W. Running *et al.*, *Bioscience* **54**, 547 (2004).
9. R. B. Myneni *et al.*, *Remote Sens. Environ.* **83**, 214 (2002).
10. M. Zhao, F. A. Heinsch, R. R. Nemani, S. W. Running, *Remote Sens. Environ.* **95**, 164 (2005).
11. M. Kanamitsu *et al.*, *Bull. Am. Meteorol. Soc.* **83**, 1631 (2002).
12. W. C. Palmer, *Research Paper 45, U.S. Dept. of Commerce* (U.S. Department of Commerce, Washington, DC, 1965).
13. A. Dai, K. E. Trenberth, T. Qian, *J. Hydrometeorol.* **5**, 1117 (2004).
14. K. A. Masarie, P. P. Tans, *J. Geophys. Res.* **100**, 11593 (1995).
15. C. D. Keeling *et al.*, *S.I.O. Reference Series No. 00-21* (Scripps Institution of Oceanography, Univ. of California, San Diego, CA, 2001).
16. E. A. Davidson, I. A. Janssens, Y. Luo, *Glob. Change Biol.* **12**, 154 (2006).
17. D. D. Baldocchi, *Aust. J. Bot.* **56**, 1 (2008).
18. G. R. van der Werf *et al.*, *Atmos. Chem. Phys.* **6**, 3423 (2006).
19. P. Ciais *et al.*, *Nature* **437**, 529 (2005).
20. O. L. Phillips *et al.*, *Science* **323**, 1344 (2009).
21. A. R. Huete *et al.*, *Geophys. Res. Lett.* **33**, L06405 (2006).
22. S. R. Saleska, K. Didan, A. R. Huete, H. R. da Rocha, *Science* **318**, 612 (2007); published online 20 September 2007 (10.1126/science.1146663).
23. A. Samanta *et al.*, *Geophys. Res. Lett.* **37**, L05401 (2010).
24. J. M. Chen *et al.*, *Geophys. Res. Lett.* **33**, L10803 (2006).
25. A. Angert *et al.*, *Proc. Natl. Acad. Sci. U.S.A.* **102**, 10823 (2005).
26. S. Piao *et al.*, *Nature* **451**, 49 (2008).
27. I. A. Janssens *et al.*, *Nat. Geosci.* **3**, 315 (2010).
28. J. L. Monteith, *Symp. Soc. Exp. Biol.* **19**, 205 (1965).
29. P. M. Cox, R. A. Betts, C. D. Jones, S. A. Spall, I. J. Totterdell, *Nature* **408**, 184 (2000).
30. I. Y. Fung, S. C. Doney, K. Lindsay, J. John, *Proc. Natl. Acad. Sci. U.S.A.* **102**, 11201 (2005).
31. P. Friedlingstein *et al.*, *J. Clim.* **19**, 3337 (2006).
32. J. G. Canadell *et al.*, in *Terrestrial Ecosystems in a Changing World*, J. G. Canadell, D. Pataki, L. Pitelka, Eds. (Springer, Berlin, 2007), pp. 59–78.
33. G. A. Meehl, C. Tebaldi, *Science* **305**, 994 (2004).
34. C. Funk *et al.*, *Proc. Natl. Acad. Sci. U.S.A.* **105**, 11081 (2008).
35. A. L. Westerling, H. G. Hidalgo, D. R. Cayan, T. W. Swetnam, *Science* **313**, 940 (2006); published online 6 July 2006 (10.1126/science.1128834).
36. C. D. Allen *et al.*, *For. Ecol. Manage.* **259**, 660 (2010).
37. W. A. Kurz *et al.*, *Nature* **452**, 987 (2008).



38. We thank the reviewers and L. Jones, C. Cleveland, and Q. Mu for helpful comments. This work would not have been possible without continuous financial support from the NASA Earth Observing System MODIS project (grant NNX08AG87A). Moreover, we gratefully acknowledge all MODIS land product science team members for their efforts in generating high-quality data sets. NCEP_Reanalysis 2 data were provided by the NOAA/OAR/Earth System Research Laboratory Physical Sciences Division, Boulder, Colorado, USA, from their Web site at www.esrl.noaa.gov/psd/.


**Supporting Online Material**

www.sciencemag.org/cgi/content/full/329/5994/940/DC1
SOM Text
Figs. S1 to S14
Tables S1 to S6
References and Notes


21 May 2010; accepted 16 July 2010
10.1126/science.1192666


# Loss of DNA Replication Control Is a Potent Inducer of Gene Amplification


**Brian M. Green,[1] Kenneth J. Finn,[2] Joachim J. Li[3]***



**Eukaryotic cells use numerous mechanisms to ensure that no segment of their DNA is inappropriately re-replicated, but the importance of this stringent control on genome stability has not been tested. Here we show that re-replication in *Saccharomyces cerevisiae* can strongly induce the initial step of gene amplification, increasing gene copy number from one to two or more. The resulting amplicons consist of large internal chromosomal segments that are bounded by Ty repetitive elements and are intrachromosomally arrayed at their endogenous locus in direct head-to-tail orientation. These re-replication–induced gene amplifications are mediated by nonallelic homologous recombination between the repetitive elements. We suggest that re-replication may be a contributor to gene copy number changes, which are important in fields such as cancer biology, evolution, and human genetics.**


A central tenet of eukaryotic cell biology is that cells replicate their DNA only once every cell cycle. Although it has become an article of faith that this regulation is important because re-replication would threaten genome stability (*1*), that faith has never been experimentally tested. Preventing re-replication in eukaryotic cells requires blocking re-initiation at thousands of origins scattered throughout the genome, and eukaryotic cells use numerous overlapping mechanisms to do this (*2*, *3*). By disrupting these mechanisms in a controlled manner, we are now able to examine re-replicated cells for possible genomic alterations.

The alterations we first looked for were heritable increases in gene copy number. Such increases are observed in the gene amplifications commonly associated with cancers (*4*, *5*), the gene duplications important for molecular evolution (*6*), and the copy number variations prevalent in human genomes (*7*). Although re-replication was once a leading model for copy number increases, specifically during gene amplification (*8*, *9*), the model has long been abandoned for lack of experimental support for it (*10*). Hence, re-replication is not seriously considered as a possible source of heritable copy number changes (*4*, *11*, *12*). Here, we demonstrate that re-replication can readily induce copy number changes, provoking reconsideration of re-replication as a potential source of such changes in cancer and evolution (*8*).

We have developed a system to detect and quantify early amplification events arising from a transient and limited pulse of re-replication at a defined genomic locus in the budding yeast *Saccharomyces cerevisiae* (Fig. 1A and figs. S1 and S2A). We took advantage of our ability to induce re-replication predominantly from a single origin (*ARS317*) by conditionally deregulating the replication initiation proteins Mcm2-7 and Cdc6 ($MC_{2A}$ genetic background) (*13*). We also adapted a copy number assay in which cells with a single copy of the *ade3-2p* allele turn pink, and cells with two or more copies turn red (*14*).

*ARS317* and *ade3-2p* were combined in a re-replicating reporter cassette (fig. S1A) that was integrated at either of two loci on chromosome IV (Chr $IV_{567kb}$ and Chr $IV_{1089kb}$) in a haploid $MC_{2A}$ background from which the endogenous *ARS317* was deleted. After arresting cells at the $G_2$/M phase [time ($t$) = 0 hours], we transiently induced re-replication until half of the *ARS317* origins re-initiated ($t$ = 3 hours), then plated for isolated colonies at both time points. The mostly pink colonies were screened for heritable amplification of *ade3-2p* by looking for colonies with red sectors (fig. S1B). Colonies with one-half, one-quarter, or one-eighth red sectors were scored to focus on amplifications arising within three generations of the re-replication pulse (table S1).

Inducing re-replication for 3 hours from the *ade3-2p-ARS317* cassette integrated at Chr $IV_{567kb}$ (strain YJL6558) caused a 42-fold increase in red sectors to 3.3% of all colonies (Fig. 1B). Suppressing this re-replication by removing deregulated Cdc6 from the $MC_{2A}$ background (YJL6974) or *ARS317* from the cassette (YJL6555) resulted, respectively, in only 4- and 12-fold increases in red sectors (Fig. 1B), most of which had not amplified the *ade3-2p* cassette. Re-replication also induced colony sectoring by 38-fold when the *ade3-2p-ARS317* cassette was relocated to Chr $IV_{1089kb}$ (fig. S2B and table S1).

Array comparative genomic hybridization (aCGH) on 35 red sectors derived from YJL6558 (table S2) confirmed that most [31 of 35 (31/35)] had at least two copies of an internal chromo-


[1]Department of Molecular Biology and Genetics, Johns Hopkins University School of Medicine, Baltimore, MD 21205, USA. [2]Department of Biochemistry and Biophysics, University of California, San Francisco (UCSF), San Francisco, CA 94158, USA. [3]Department of Microbiology and Immunology, UCSF, San Francisco, CA 94158, USA.

*To whom correspondence should be addressed. E-mail: joachim.li@ucsf.edu